

Model Experiments of an Offshore Supply Vessel Running in Astern Waves



Naoya Umeda, Sreenath Subramaniam, Aqmil Alway, Akihiko Matsuda, Atsuo Maki, Satoshi Usada, and Daisuke Terada

Abstract At the IMO (International Maritime Organization), the second generation intact stability criteria for pure loss of stability was developed in 2020. In its interim guidelines (IMO in “Interim Guidelines on the Second Generation Intact Stability Criteria”, MSC.1/Circ. 1627, 2020 [2]), vessels with extended low weather deck such as offshore supply vessels (OSVs) are exempted from this application, but its background has not yet been explained other than a sample calculation resulting in inconsistencies between different criteria levels. To solve this problem, the authors executed model experiments for a typical OSV in astern waves. The test results demonstrated that the phenomenon assumed by the pure loss of stability criteria is not pertinent to the OSV. Instead, it is the phenomenon which occurs due to trapped water on deck which seems to be of greater relevance for the stability of the OSV in astern seas. The effect of low weather deck length was also investigated by systematically modifying hull forms with the help of CAD software. Further, the on-deck trapped water behaviour was also studied in a separate series of model experiments involving direct measurement of the changing deck water level. The tests confirmed that the

N. Umeda · S. Subramaniam (✉) · A. Maki · S. Usada
Osaka University, Suita, Japan
e-mail: sreenath_subramaniam@naoe.eng.osaka-u.ac.jp

N. Umeda
e-mail: umeda@naoe.eng.osaka-u.ac.jp

A. Maki
e-mail: maki@naoe.eng.osaka-u.ac.jp

A. Alway
NAPA Japan, Kobe, Japan
e-mail: Aqmil.Alway@napa.fi

A. Matsuda
Japan Fisheries Research and Education Agency, Kamisu, Japan
e-mail: amatsuda@fra.affrc.go.jp

D. Terada
National Defense Academy of Japan, Yokosuka, Japan
e-mail: dterada@nda.ac.jp

trapped water can induce both static and dynamic moments depending on the speed of the vessel and the wave conditions.

Keywords IMO · Second generation intact stability criteria · Pure loss of stability · Water on deck · Offshore Supply Vessel

1 Introduction

The second generation intact stability criteria developed by the IMO [2] are intended to cover stability failure due to pure loss of stability in following and stern quartering waves [7]. For this failure mode, the direct stability assessment and two-level vulnerability criteria should be applied. As a possible tool for the direct stability assessment, a coupled surge-sway-yaw-roll numerical model in irregular waves was developed and validated with model experiments using a containership [5].

Based on the knowledge obtained from this numerical model, the level 1 and 2 vulnerability criteria were developed [2]. Here the level 1 and 2 criteria utilise GM and GZ in longitudinal waves, respectively. The standards of these criteria were determined to avoid the “false negative” problem between the two levels utilising many sample calculation results which did not include offshore supply vessels [1]. The sample calculations executed by the delegations from Japan and China, [4] indicate that offshore supply vessels easily comply with the level 1 but do not comply with the level 2 criterion. This inconsistency is a so-called “false negative” problem, which should be avoided in regulatory applications. Thus, the interim vulnerability criteria [2] are not allowed to be applied to “a vessel with extended low weather deck due to increased likelihood of water on deck or deck-in-water”.

However, the definition of the extended low weather deck, based on a model experiment or equivalent, has not yet been established. Published free-running model experiments of OSVs in astern waves were also not available. Therefore, the authors executed the first set of model experiments in 2015, using a scaled model of typical offshore supply vessel in stern quartering waves and compared the measured results with the second generation intact stability criteria. As a result, the reasons why OSVs should be exempted from the application of the pure loss of stability criteria are revealed. In order to investigate the effect of weather deck length, calculations of the vulnerability criteria were conducted by systematically modifying the above-water hull forms of the offshore supply vessel using CAD software, i.e. the NAPA software.

Further, the assumptions regarding the behaviour of trapped water on deck from the model experiments conducted in 2015 were confirmed in a second set of model experiments carried out in 2019, short summary of these experiments are available in Subramaniam et al. [6]. This additional set of model runs involved the direct measurement of the changing deck water level using camera and pressure sensors. The second set of experiments was also separated into two stages. Stage 1 runs were carried out with the openings, i.e. aft end and freeing ports opened, similar to 2015

model experiments. Stage 2 runs were carried out with closed openings and deck filled in advance with a constant amount of water. These additional free running model test data confirmed that the trapped water can act as a kind of anti-rolling tank around the service speed of the vessel.

2 Subject Ship and Model Experiments

The first set of free-running model experiments of the 60 m long offshore supply vessel (OSV), as shown in Figs. 1 and 2, in stern quartering waves were conducted at a seakeeping and manoeuvring basin of the National Research Institute of Fisheries Engineering of Japan in 2015. The vessel has a deckhouse forward and a low weather deck situated from its midship to its stern with bulwarks and freeing ports. The length of the low weather deck is 40 m in full scale. The service Froude number of the vessel is 0.3 and the vessel is equipped with twin propellers and twin rudders. Its principal particulars and righting arm curve are shown in Table 1 and Fig. 3, respectively. The metacentric height is set to marginally comply with level 2 criteria for pure loss of stability, which is lower than the designed one. The vessel under the experimental condition is judged not to be vulnerable to pure loss of stability according to the level 1 criterion because the GM with the wave steepness of 0.0334 is 1.32 m, which is much larger than the standard of 0.05 m. However, the OSV is regarded as critical with the level 2 criterion having CR value of 0.06. Thus, an inconsistency between the two levels could appear if the calm-water GM is smaller than 1.45 m.

The vessel model ran with a constant propeller speed (revolutions per minute) and attempted to keep its specified course with a PD autopilot in stern quartering waves. The translational and rotational motions of the vessel model were measured with an optical tracking system, consisting of two theodolites and two prisms, and an optical-fibre gyroscope, respectively.

For the second set of free running model tests conducted in 2019, the same model as the 2015 model experiments was utilised. In this experiment, the vertical position

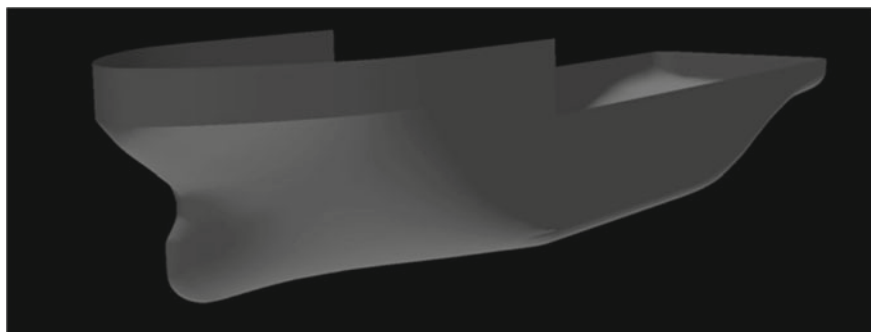


Fig. 1 3D view of the hull form of the used OSV



Fig. 2 Free-running model experiment of the OSV in stern quartering waves executed in 2015

Table 1 Principal particulars of the OSV

Items	Ship	Model
Length between perpendiculars (L_{pp})	60.00 m	2.00 m
Moulded breadth	16.40 m	0.547 m
Moulded depth	7.20 m	0.24 m
Moulded draught	6.00 m	0.20 m
Metacentric height (GM)	1.45 m	0.0483 m
Natural roll period	11.50 s	2.10 s

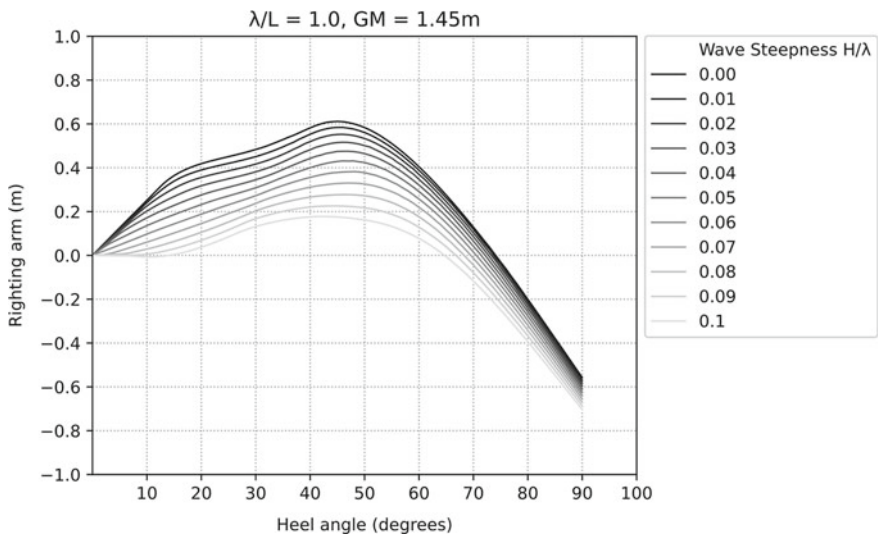


Fig. 3 GZ curve of the OSV with a wave crest amidship in longitudinal waves. Here the wavelength is equal to the ship length, and the wave steepness ranges from 0 to 0.1

of the casing of the steering gears at the aft end was moved from the weather deck to the bulwark height, to allow more free movement of water on the deck, as shown in Figs. 2 and 4. Also, apart from the conventional system for free-running model experiments, additional systems were used to continuously monitor the changing deck water level. This additional system included a set of 5 cameras and 4 pressure sensors. Four cameras were positioned at the four corners of the weather deck, and one camera was placed at the forecabin with a clear view of the deck. Linear scales were placed opposite each camera placed on the weather deck to note the changing water level. The four pressure sensors were placed adjacent to the linear scale: the measured pressure was converted into the head of water. The arrangement can be seen in Figs. 4 and 5. The second set of experiments was also executed with closed openings trapping a constant amount of water on deck (Stage 2) to isolate the water on deck phenomenon, other than the approach of the experiment in 2015 (Stage 1).

The model was released when waves were sufficiently propagated in the water area of the basin. These experimental procedures are based on the ITTC (International Towing Tank Conference) recommended procedures for intact stability model test [3].

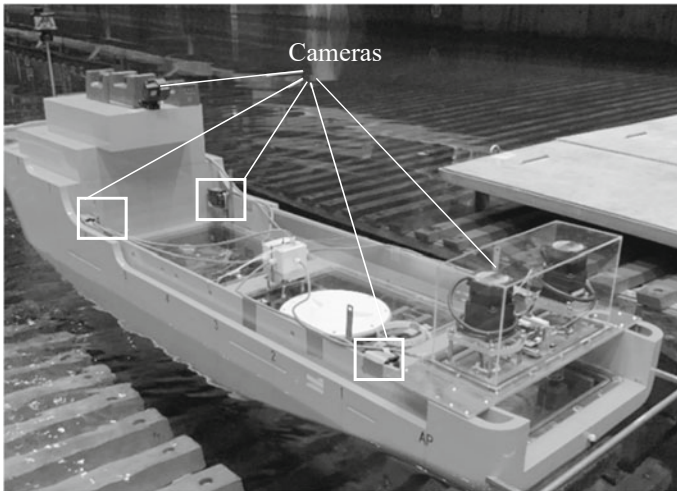
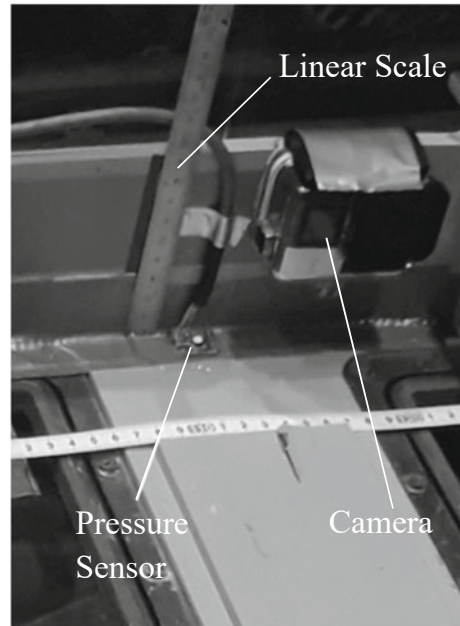


Fig. 4 Model and camera arrangement of the model experiment in 2019

Fig. 5 Camera and pressure sensor arrangement of the model experiment in 2019



3 Experimental Results and Discussions

3.1 2015 Model Experiment

The maximum roll angles measured during each model run in astern waves are shown in Fig. 6. Here the wavelength is equal to the ship length, as the worst case assumed in the criteria for pure loss of stability and the nominal Froude number ranges from 0.24 to 0.37 as also specified by the criteria. The used wave steepness H/λ , are 0.03, 0.05 and 0.1. The results indicate that roll angles under these wave and operational conditions are smaller than 15° so that no real danger can be expected. While for a normal ship running in astern waves the roll response increases with the increasing ship speed (e.g. [2, 5]), this particular ship shows a different trend with respected to speed.

The reason presumed was that the trapped water-on-deck acted as a kind of anti-rolling tank, partly because the estimated natural period of possible trapped water on deck, which ranges between 1.8 s and 2.4 s in model scale as shown in Fig. 7, is comparable to the natural roll period of 2.1 s. The roll decay test of this model in calm water with large instantaneous initial roll angle (enabling water to ingress into the deck via the openings), was rapidly damped, as shown in Fig. 8. Thus, we can presume that this large roll damping is due to resonance of the ship roll motion and the trapped water on deck. It is similar to a mechanism of an anti-rolling tank.

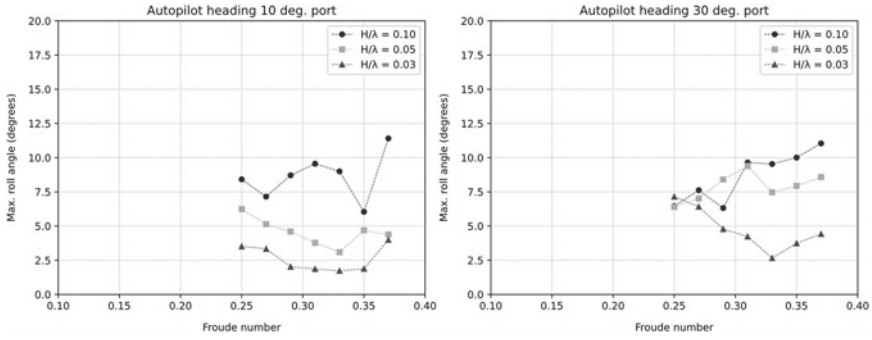


Fig. 6 Maximum roll angles (in degrees) recorded in the experiment for the wavelength to ship length ratio (λ/L) of 1.0 and the wave steepness (H/λ) of 0.03, 0.05 and 0.1 with the autopilot headings of 10 and 30° port from the wave direction

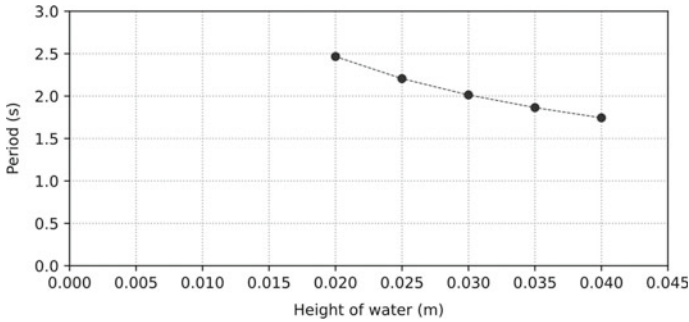


Fig. 7 Estimated natural period of trapped water on deck as a function of water depth on deck

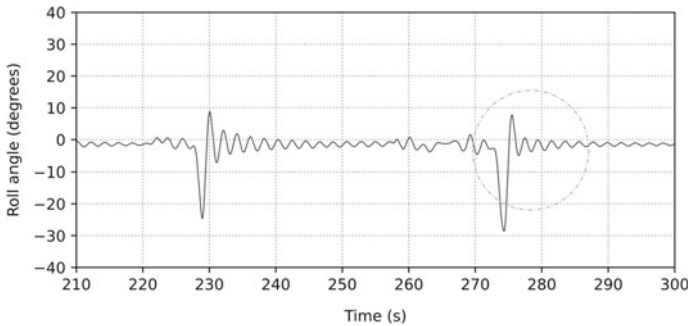
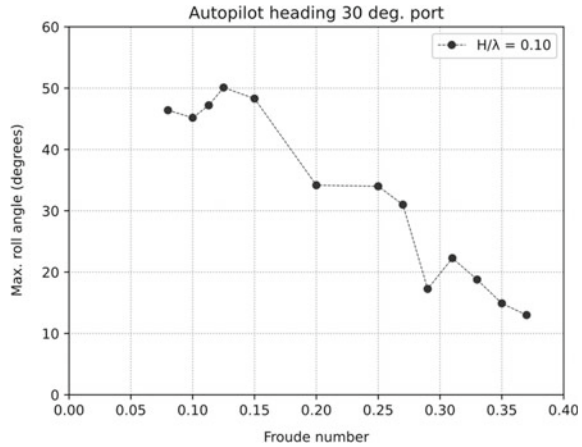


Fig. 8 Time series of roll decay test with the large instantaneous initial roll angle in degrees

Fig. 9 Maximum roll angles (in degrees) recorded during each free running test for the wavelength to ship length ratio (λ/L) of 1.5 and wave steepness (H/λ) of 0.1 with the autopilot heading of 30° port from the wave direction



As a next step, model runs were conducted with longer waves. Here the ratio of wavelength to ship length, λ/L , was 1.5, and the wave steepness was 0.1. In this case, larger water volume was trapped on deck because water ingress across the bulwarks exceeds egress through the freeing ports. The results shown in Fig. 9 indicate that larger roll angles, such as about 50°, were recorded. When the speed decreased, the roll angle increased. This tendency is entirely different from the pure loss of stability.

The reason for the larger roll could be the heeling moment of trapped water-on-deck, which could depend on the height of bulwarks. In the case of this OSV, if the roll angle exceeds about 21°, the relative water level exceeds the bulwark (bulwark submerged). From the GZ curve for this wavelength shown in Fig. 10, it can be observed that the loll angle is almost 20° and the angle of vanishing stability is slightly larger than 50°. Thus, the bulwark submergence cannot be avoided with wave crest amidship as the OSV will roll to the loll angle and submerge the bulwark. Then the maximum roll angle could be 50°. This suggests that the reason for large roll seems to be hydrostatic heel moment due to water on deck.

3.2 2019 Model Experiments

Maximum Roll angles

The maximum roll angles observed during the free runs carried out in Stage 1 are shown in Fig. 11. In Stage 1, the model run was executed with all the weather deck openings opened, and there was water ingress and egress, so the results include the complete water on deck phenomenon. The ratio of wavelength to ship length, λ/L , was set as 1.5. Figure 11 indicates that trends exist in the maximum roll angle when the larger wave steepness of $H/\lambda = 0.1$ is used. It is the result of a significant amount of water getting trapped in the weather deck due to steep waves.

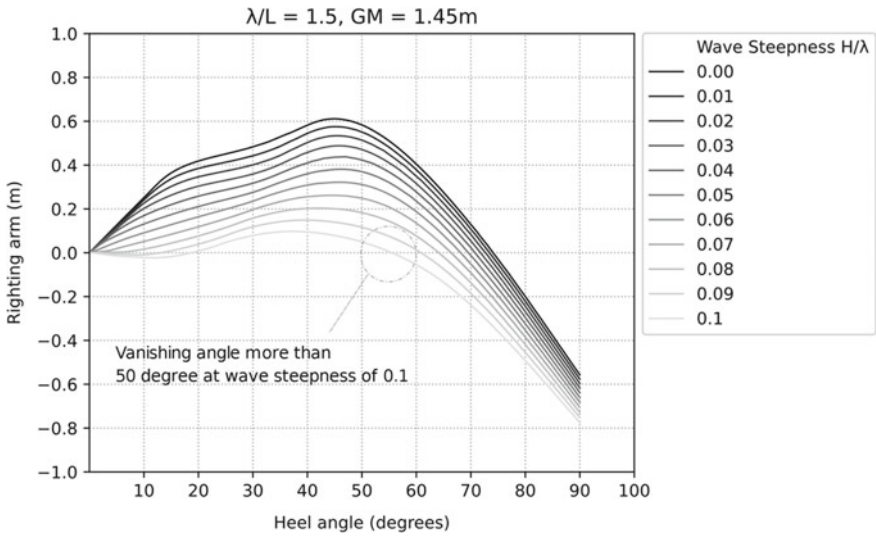


Fig. 10 GZ curve of the OSV at a wave crest amidship in longitudinal waves for the wavelength to ship length ratio, λ/L of 1.5 and the wave steepness ranges from 0 to 0.1

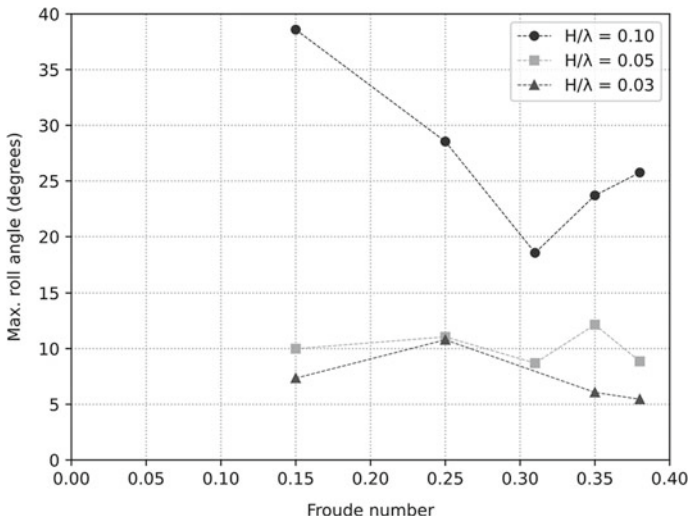


Fig. 11 Maximum roll angle vs Froude number for $\lambda/L = 1.5$ and autopilot heading relative to waves = 30° port (Stage 1, all openings open)

At low speed, the roll angle is very high since much water enters the ship from the stern opening and causes a large static heeling moment. When the speed of the vessel increases, the encounter frequency of the waves decreases and the average amount of trapped water decreases because of reduced ingress from the stern opening, so the maximum roll angle decreases. The increase in damping caused by the trapped water could be another reason for the decrease in roll angle. However, when the Froude number exceeds 0.31, the maximum roll angle again increases. The primary reason for this increase in roll angle is the near in-phase motion of the water with the low frequency ship roll. Roll restoring variation and yaw-roll coupling [5] could be secondary effects contributing to the increase in the roll angle for this vessel.

Comparison of the 2015 and 2019 model experiments for the same wave conditions of $\lambda/L = 1.5$ and $H/\lambda = 0.1$ (Figs. 9 and 11), shows both similarities and differences. For the case of lower Froude numbers, the maximum roll angle variation is similar for both Figs. 9 and 11, as the maximum roll angle is mainly governed by the amount of water entering over the bulwark from the sides. But for higher speeds (above F_n 0.31) the variation of maximum roll angle is different in the two figures, this is because at higher speeds the entry of water from the stern becomes important. For the 2019 model experiments since the steering gear location was raised, water could more easily ingress from the aft. The motion of this trapped water nearly in phase with the low frequency ship roll motion, may have caused an increase in the roll angle at higher speeds for the 2019 model experiments.

In order to investigate the effect of initial yaw on the maximum roll angles we carried out an additional set of free runs for the case of $H/\lambda = 0.1$ and $\lambda/L = 1.5$, with a smaller initial yaw. The results are shown in Fig. 12. For lower Froude numbers maximum roll angle is almost the same irrespective of the initial yaw, as the deck is saturated with a large amount of water. At higher Froude numbers (above 0.31) the maximum roll angle is slightly larger with a smaller initial yaw. This could be due to the initial increased ingress of water from the stern compared to the case with larger initial yaw. The trends of variation of maximum roll angles is however similar for both cases.

Figure 13 shows the variation of maximum roll with Froude number during Stage 2 with closed openings. Free running model tests were executed with the deck both empty and pre-filled with a known amount of water. Result from the latter contains the ship motion along with the deck water motion behaviour; water inflow and outflow through the openings are absent. In these cases, the ratio of wavelength to ship length, λ/L , was set as 1.5 but a smaller wave steepness of $H/\lambda = 0.03$ was used to avoid additional water shipping over the bulwarks.

For the case of amount of water filled on deck equal to 2.23% of ship mass, the initial drop in the maximum roll angle from the Froude number of 0.15–0.31 may be attributed to the increase in the roll damping and a further increase in the maximum roll beyond the Froude number of 0.31 may be attributed to the near in phase motion of water with ship roll and secondary effects of roll restoring variation or yaw-roll coupling.

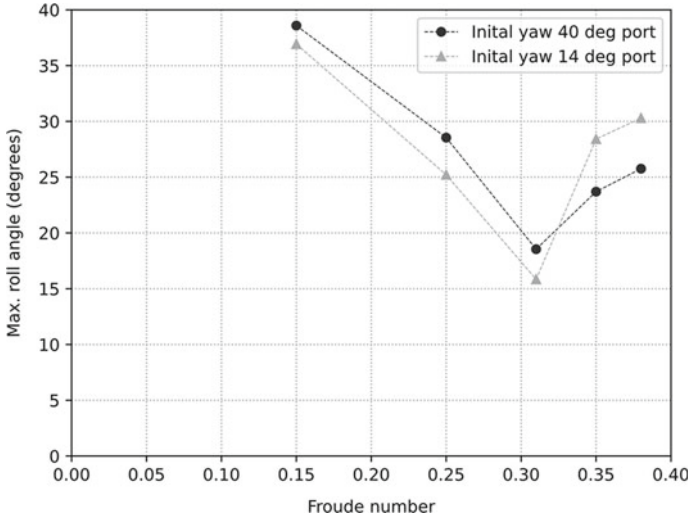


Fig. 12 Maximum roll angle versus Froude number for $\lambda/L = 1.5$, $H/\lambda = 0.1$, autopilot heading relative to waves = 30° port and initial yaw angles of 14 and 40° port (Stage 1, all openings open)

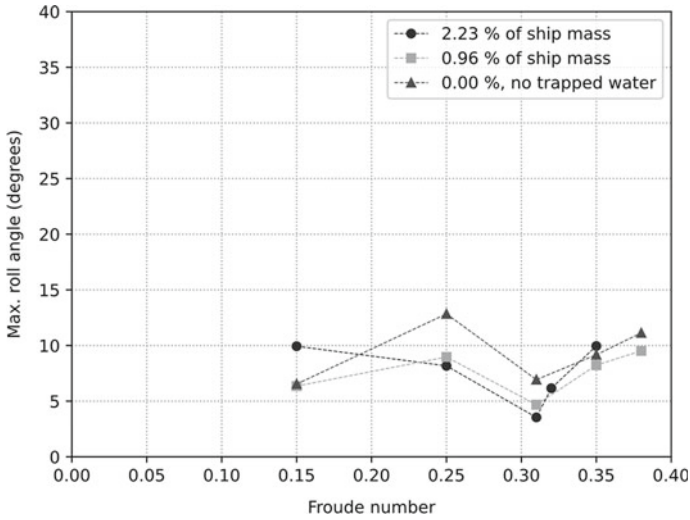


Fig. 13 Maximum roll angle versus Froude number for $\lambda/L = 1.5$, $H/\lambda = 0.03$ and autopilot heading relative to waves = 30° port (Stage 2, all openings closed and deck is filled in advance with a known amount of water as a percentage of ship mass)

Damping caused by water trapped on the deck

The confirmation of the presence of damping was obtained by analysing the results of Stage 2 free-running data from the 2019 model experiments. The results with the larger amount of trapped water (2.23% of ship mass) were utilised. Here all the openings were closed, and the amount of water inside the deck was constant throughout the model run. Thus, the initial decrease in the maximum roll angle could be attributed to roll damping caused by the water on deck. Time histories of the varying deck water level and the ship roll motion were compared to check the phase difference between the two. The time difference between a peak of roll angle on starboard/port side and the corresponding water level peak of the same side was calculated and converted to the phase difference using the average frequency of ship roll and water motion. Figure 14 show the time histories of ship roll and water motion for the Froude number of 0.31 and the phase difference. Figure 15 shows the change of the phase difference between water motion and ship roll with ship speed. It can be seen that the phase difference is close to 90° between the Froude number 0.25 and 0.31. The damping effect due to deck water motion is highest in this region. The phase difference further decreases with increasing speed.

The reason why the damping effect is at the maximum when the phase difference between ship motion and water motion is 90° is explained in Fig. 16. In Fig. 16a the ship roll angle is the largest towards starboard and the water is moving towards starboard. It induces no roll moment due to the water on deck. In Fig. 16b the ship is rolling to port and the water trapped is on the starboard side, which induces a roll moment in the opposite direction to the roll velocity. Similar explanations can

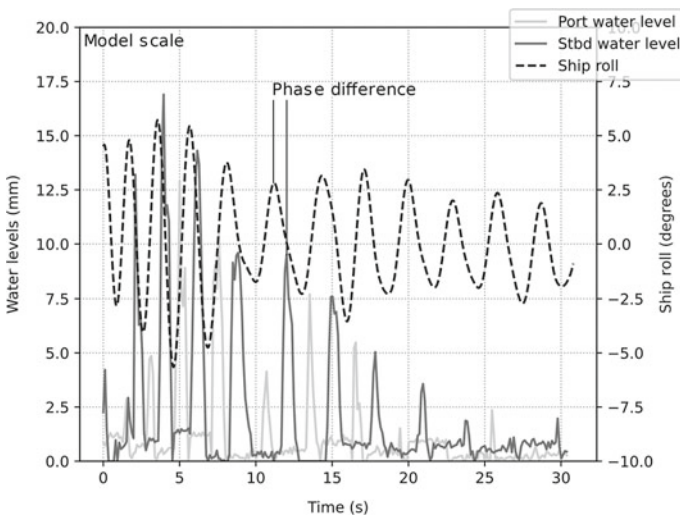


Fig. 14 Time history of ship roll and water levels for $F_n = 0.31$, $\lambda/L = 1.5$, $H/\lambda = 0.03$ and autopilot heading relative to waves = 30° port (Stage 2, all openings closed but the deck is filled in advance with a known amount of water, 2.23% of ship mass)

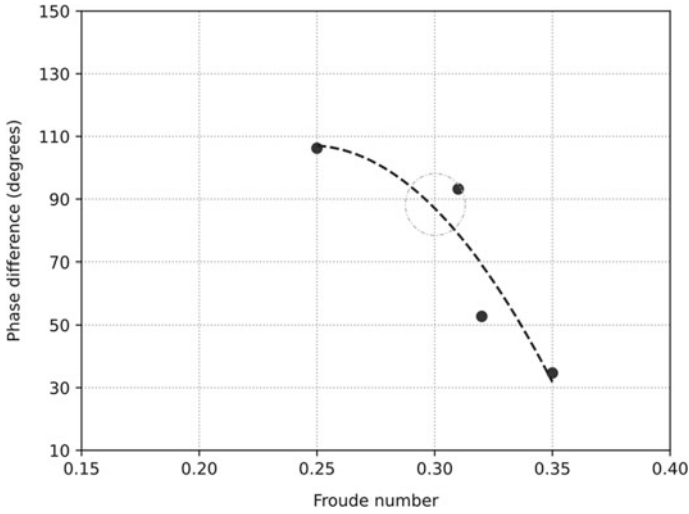


Fig. 15 Phase difference between motion of trapped water on deck and ship roll angle versus Froude number

be provided for the Fig. 16c and d. The maximum roll moment due to water and maximum roll velocity are out of phase; in other words, the phase difference between the ship roll and the water motion is 90°.

4 Numerical Simulations

4.1 Free Running Simulations

Numerical simulations were carried out based on the data from the 2015 model experiments. For investigating the mechanism of this dangerous phenomenon, the coupled surge-sway-yaw-roll numerical model proposed by Kubo et al. [5] was used for simulating the dynamic behaviour under the wave conditions used in the experiment. This is a manoeuvring-type model with linear wave exciting forces and restoring variation focusing on low-frequency phenomena, but the effect of trapped water on the deck is not considered in the first attempt. All propulsion and manoeuvring coefficients input for the simulation model are estimated from conventional captive model experiments. The linear wave exciting forces and restoring variation were calculated by a slender body theory with low encounter frequency assumption and a direct pressure integral of incident wave pressure up to instantaneous water level, respectively.

The comparisons between the experiments and the simulations are shown in Figs. 17 and 18. For the case with the Froude number of 0.31 shown in Fig. 17, the measured and calculated roll periods are 14.80 s and 17.68 s respectively. The

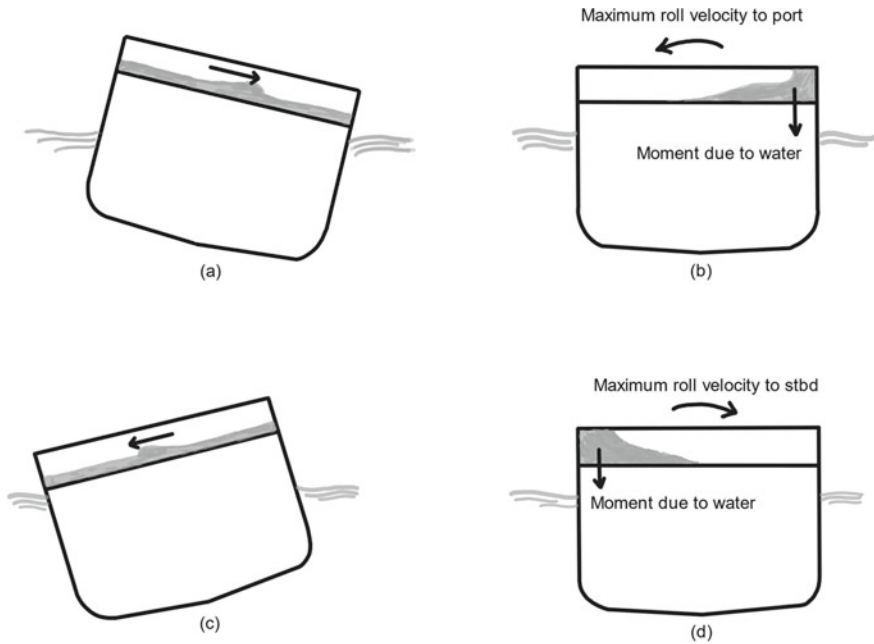


Fig. 16 Phase difference between motion of trapped water on deck and ship motion

encounter wave period (calculated using the average yaw and average surge velocity) is 15.29 s. The natural roll period of the system without water is 11.5 s. The measured roll amplitude is much smaller than the calculated one so that the trapped water, which is not included in the numerical model, has a role to damp the roll motion as a kind of anti-rolling tank.

For the lower speed case of the Froude number of 0.125 shown in Fig. 18, the measured and calculated roll period are 20.80 s and 10.23 s respectively. The encounter wave period is 10.84 s so that the period doubling of roll motion was identified in the experiment. The measured roll amplitude is much larger than the simulated one. Furthermore, the mean of the measured roll angle is also larger than that of the calculated roll angle. This suggests that hydrostatic heel moment due to trapped water on deck, which is not included in the numerical model, has a crucial role for inducing the extremely large roll angle in the experiment. The large amount of water trapped on the deck could result not only in large mean roll angle but also in large roll amplitude due to the varying restoring moment due to the relative ship position to overtaking waves.

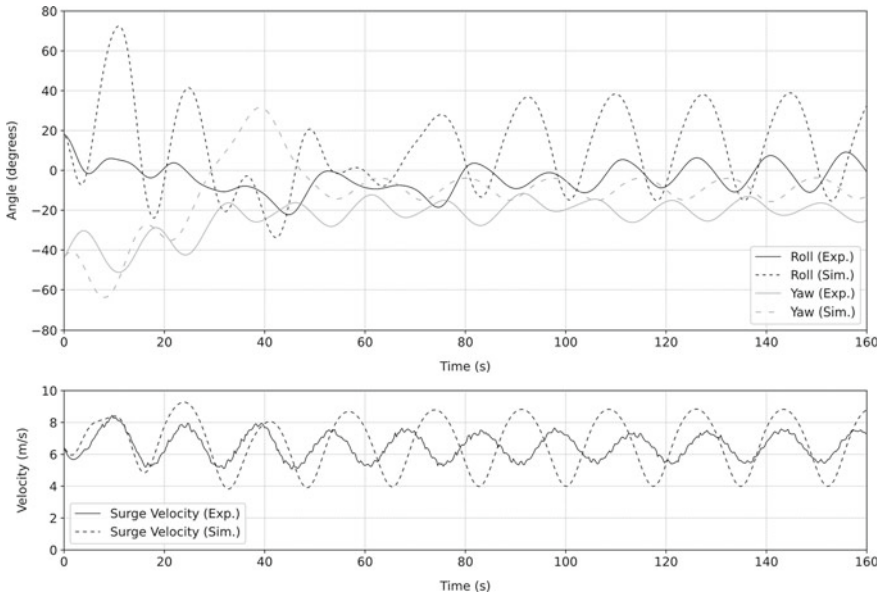


Fig. 17 Comparison between the simulation and the experiment for the wave steepness (H/λ) of 0.1, the wavelength to ship length ratio (λ/L) of 1.5, the nominal Froude number is 0.31, the specific heading angle from the wave direction of 30° and the rudder gain of 3.0. Here the positive roll means starboard side down and the positive yaw does starboard turn

4.2 Effect of Weather Deck Length

For creating a proper definition of a vessel with extended low weather deck, the NAPA system was used to make systematically modified hulls of our offshore supply vessel (OSV) model.

The weather deck length, as defined in Fig. 19, was systematically modified by extending the forecastle deck towards the aft while keeping other dimensions constant. The displacement, draft and trim of the vessel was assumed to remain unchanged during the process. Then the level 1 and 2 criteria were applied to the generated hulls. All modified hulls comply with the level 1 criteria with directly calculated GM in waves exceeding the required value of 0.05 m. The level 2 criteria consist of two requirements: CR1 is based on the angle of vanishing stability, and CR2 is based on the angle of the heel under the action of the speed-dependent heeling lever. The standard for these values is 0.06. Here the Froude number is set to be 0.25. The results are shown in Fig. 20.

When the weather deck length is larger than half the length between perpendiculars, the CR2 value rapidly increases so that the vessel is judged as vulnerable to pure loss of stability. However, the vessel is not so relevant to the danger due to pure loss of stability as mentioned before. To avoid such “false negative” case, it can be

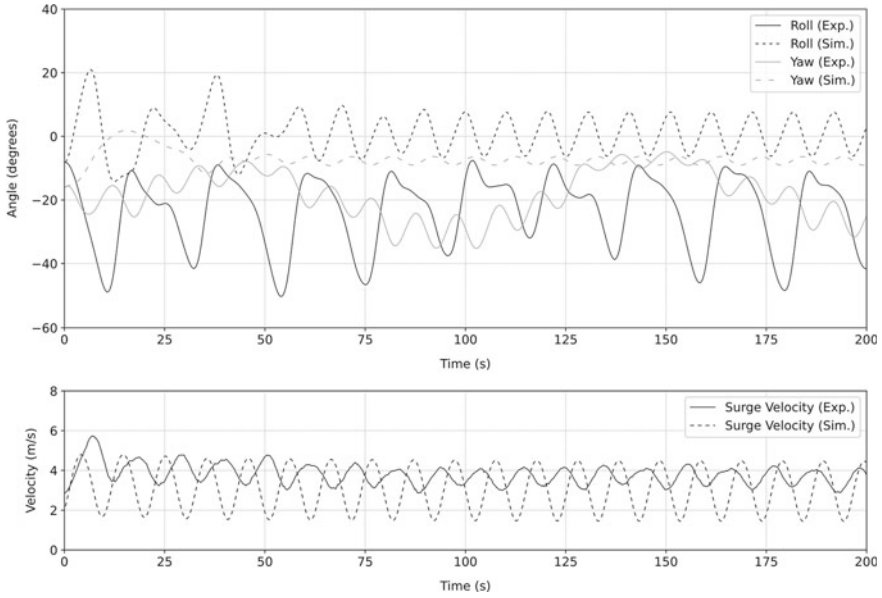


Fig. 18 Comparison between the simulation and the experiment for the wave steepness (H/λ) of 0.1, the wavelength to ship length ratio (λ/L) of 1.5, the nominal Froude number is 0.125, the specific heading angle from the wave direction of 30° and the rudder gain of 3.0

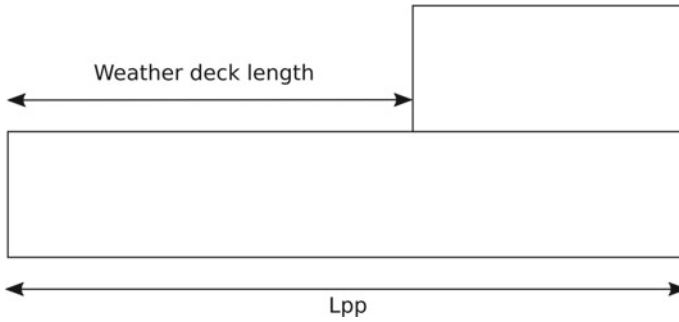


Fig. 19 Simplified OSV with weather deck length definition

recommended to include the low weather deck length in the definition of a vessel with extended low weather deck.

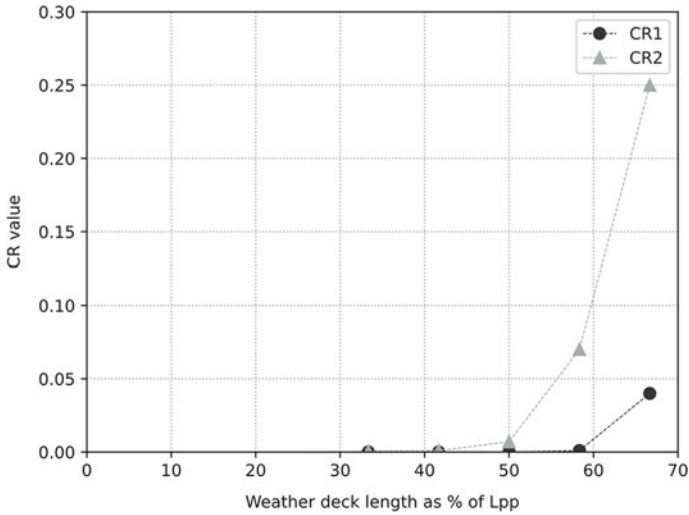


Fig. 20 Weather deck length and CR values from Level 2 criteria results

5 Conclusions

Two separate model experiments were carried out to study the behaviour of the OSV in astern waves, and from both the experiments it is clear that the water on deck effect plays a major role in the vessel’s roll motion. The following main conclusions can be drawn:

- When the wave conditions are such that the water ingress is significant ($\lambda/L = 1.5$ and $H/\lambda = 0.1$),
 - At lower Froude numbers, the maximum roll angle could be very high, close to the angle of vanishing stability. This is due to the large static heeling moment caused by the significant amount of water trapped on one side of the weather deck.
 - As the speed of the vessel increases, the maximum roll angle decreases due to the combined effect of reduced water ingress, and roll damping due to trapped water. This tendency is different from the pure loss of stability.
 - At very high Froude number (above 0.31), the maximum roll angle again starts to increase due to the near in-phase motion of water with the low frequency ship roll. Roll restoring variation and yaw-roll coupling could be secondary effects contributing to the increase in roll angle.
- When the wave conditions are such that the water ingress is less ($\lambda/L = 1.0$ and $H/\lambda = 0.1, 0.05, 0.03$; $\lambda/L = 1.5$ and $H/\lambda = 0.05, 0.03$),
 - The amount of water trapped inside is small and the ship can easily roll with reduced amounts of water. The roll frequency is high at low Froude number

and it reduces as the ship speed increases. Thus, the phase difference between ship motion and trapped water motion would be high at low Froude number and would decrease as the ship speed increases. The damping effect would be most effective when the phase difference approaches 90° .

- At very high Froude number, the near in phase motion of deck water and ship roll contributes to the increase in the maximum roll angle.
- Based on the systematic hull modification survey, it also can be concluded here that, if the length of low weather deck is greater than $0.5L_{pp}$, it is not appropriate to apply the level 2 pure loss criterion to this type of ships. As mentioned before, the vessel used here is not so relevant to the danger due to pure loss of stability.

Acknowledgements This work was supported by Grant-in Aids for Scientific Research from the Japan Society for Promotion of Science (JSPS KAKENHI Grant Numbers 15H02327 and 19H02360). It was partly carried out as a research activity of Goal-based Stability Criteria Project of Japan Ship Technology Research Association in the fiscal years of 2015 and 2019 funded by the Nippon Foundation. It was also a part of the collaborative research on intact stability between NAPA Japan and Osaka University. The authors sincerely thank these organisations. This is an updated version of the paper read at the 15th International Ship Stability Workshop [8] with additional research outcomes [6].

References

1. IMO (2015) Report of the working group (Part 1), SDC 2/WP.4
2. IMO (2020) Interim guidelines on the second generation intact stability criteria. MSC.1/Circ. 1627
3. ITTC (2008) Recommended procedures and guidelines, model test on intact stability; 7.5-02-07-04.1 Revision 2
4. IMO (2018) Information collected by the correspondence group on intact stability, submitted by Japan, SDC 5/6/INF.4
5. Kubo H, Umeda N, Yamane K, Matsuda A (2012) Pure loss of stability in astern seas—is it really pure? In: Proceedings of the 6th Asia-Pacific workshop on marine hydrodynamics-APHydro2012, pp 307–312
6. Subramaniam S, Umeda N, Maki A, Matsuda A (2020) Systematic experimental study on water on deck effect of an offshore supply vessel in stern quartering waves. In: Conference proceedings of the Japan society of naval architects and ocean engineers, vol 30, pp 623–627
7. Umeda N, Francescutto A (2016) Current state of the second generation intact stability criteria—achievements and remaining issues. In: Proceedings of the 15th international ship stability workshop, pp 1–7
8. Umeda N, Alway A, Usada S, Matsuda A, Terada D (2016) Model experiment of an offshore supply vessel running in astern waves, In Proceedings of the 15th Ship Stability Workshop, pp 11–16